Vapor Phase Loading of an Ionic Liquid into a Zeolitic Imidazolate Framework

Obst, Martin; Tietze, Max; Matavž, Aleksander; Rodriguez-Hermida, Sabina; Marcoen, Kristof; Hauffman, Tom; Ameloot, Rob

Published in:
Inorg. Chem.

DOI:
10.1021/acs.inorgchem.2c02615

Publication date:
2022

License:
Unspecified

Document Version:
Accepted author manuscript

Vapor-Phase Loading of an Ionic Liquid into a Zeolitic Imidazolate Framework

Martin Obst[1], Max L. Tietze[1], Aleksander Matavž[1], Sabina Rodriguez-Hermida[1], Kristof Marcoen[2], Tom Hauffman[2], Rob Ameloot[1]*

[1]Center for Membrane Separations, Adsorption, Catalysis, and Spectroscopy (cMACS), KU Leuven, Celestijnenlaan 200F, 3001 Leuven, Belgium.

[2]Research Group of Electrochemical and Surface Engineering (SURF), Vrije Universiteit Brussel, Pleinlaan 2, 1050 Brussels, Belgium.

Keywords: ionic liquid; metal-organic framework; composite; vapor phase; ship-in-bottle method

Abstract: Composites formed by a metal-organic framework (MOF) and an ionic liquid (IL) are potentially interesting materials for applications ranging from gas separation to electrochemical devices. Consequently, there is a need for robust and low-cost preparation procedures that are compatible with the desired application. We herein report a solvent-free, one-step, vapor-based ship-in-bottle synthesis of the IL@MOF composite 1-butyl-3-methylimidazolium bromide@ZIF-8 in powder and thin film forms. In this approach, volatile IL precursors are evaporated and subsequently adsorb and react within the MOF cages to form the IL.

INTRODUCTION

Incorporation of an ionic liquid (IL) into the pores of a metal-organic framework (MOF) leads to composites with potential applications in gas separation and storage, catalysis, and electrochemical devices.[1–4] Since IL@MOF composites combine the properties of MOFs and ILs, their adsorption properties and ionic conductivity can be changed considerably compared to the parent MOF material.[1] For instance, the composite [bmim]PF_6@ZIF-8 shows double the CO_2/N_2 adsorption selectivity compared to ZIF-8.[5] Ionic conductivity even below the IL freezing temperature is achieved by incorporation of [emim]NTf_2 into ZIF-8.[6] Incorporation of an IL can also render the MOF meltable, as demonstrated for [emim]NTf_2@ZIF-8.[7] Moreover, IL@MOF catalysts can be easily separated from the reaction mixture, while this is not possible for pure ILs.[1,8]

Three major approaches are followed for the preparation of IL@MOF composites: (i) IL diffusion into the MOF pores (i.e., wet impregnation in a solvent or solvent-free mixing using mortar and pestle);[9–16] (ii) ionothermal synthesis of the MOF, in which the IL acts both as a solvent and structure-directing agent, and either the anion or cation is incorporated in the pores;[17–21] and (iii) the ship-in-bottle (SIB) method,[22–25] in which the IL is formed inside the MOF pores. Among these methods, the SIB method is particularly favorable because, for a well-chosen guest-host pair, it can overcome the problem of IL leaching from the MOF. In this approach, small IL precursors are sequentially diffused into the pores, where they react to form the IL. The latter becomes sterically trapped when it is larger than the pore aperture.[1] So far, the SIB method has been only performed in solution or in neat liquid precursor.

A drawback common to all preparation methods reported thus far is that they are liquid-phase processes, requiring a solvent or a relatively large volume of precursor or IL. Furthermore, high IL loadings may be difficult to achieve due to competition with solvent molecules.[26] On the other

hand, loading of guest molecules into a MOF can be simply performed from the vapor phase. Examples are the confinement of anthracene into ZIF-8 by sublimation[26] and the loading of organometallic compounds such as ferrocene into MOF-5.[27] However, the direct loading of ILs into a MOF from the vapor phase is impractical because of their low vapor pressure ($< 10^{-3}$ mbar at moderate temperatures), and the requirement of an ultra-high vacuum ($< 10^{-8}$ mbar).[28,29] Nevertheless, several common ILs can be easily synthesized from volatile precursors. For example, imidazolium ILs are formed by the quaternization of an imidazole with an alkyl halide, even under solvent-free conditions and at moderate temperatures.[30,31] Recently, we exploited this reaction to develop the chemical vapor deposition of ILs on surfaces, resulting in ionogel thin films and patterns.[32] In that study, two volatile precursors were sequentially evaporated and diffused into a polymer film, where they reacted to form the IL. The polymer acted as a reservoir for the precursors and allowed area-selective ionogel formation. In this work, we expanded this approach to load the IL 1-butyl-3-methylimidazolium bromide ([bmim]Br) into ZIF-8 powder and thin film via a novel vapor-phase ship-in-bottle (VSIB) method (Figure 1a).

RESULTS AND DISCUSSION

ZIF-8 consists of Zn^{2+} ions connected by 2-methylimidazolate linkers. The framework has a sodalite topology consisting of 11.6 Å cages connected by small apertures of 3.4 Å.[26] Because of this topology, large molecules formed through the SIB method can be trapped inside the cages, resulting in a stable IL@MOF composite. For example, [bmim]Br has been loaded into ZIF-8 using the conventional, liquid-phase SIB method by sequentially suspending the MOF powder in the neat precursors 1-methylimidazole and 1-bromobutane.[23] In this study, [bmim]Br was selected

as target IL because both precursors are liquids with considerable vapor pressure and readily react by quaternization of the non-methylated imidazole nitrogen atom.

ZIF-8 crystals with a particle size below 1 µm were synthesized by a solvent-free method, by heating a physical mixture of zinc oxide and 2-methylimidazole.[33] The ZIF-8 powder was then placed in a Schlenk flask together with the IL precursors in separate glass boats (Figures 1b, S1). The Schlenk flask was heated to 70 °C for 20 h to allow precursor evaporation, simultaneous diffusion into the MOF powder, and subsequent reaction to form the IL.

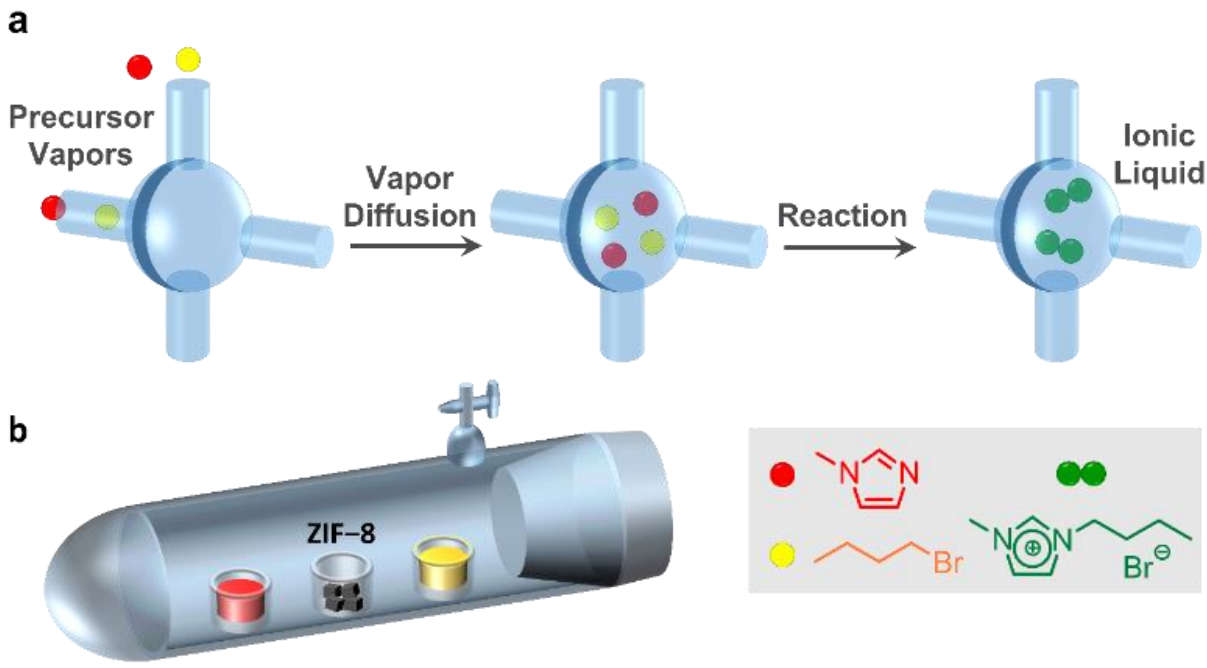

Figure 1. Vapor-phase ship-in-bottle (VSIB) method. (a) Schematic representation of the VSIB method in a MOF pore. Note the simultaneous introduction of both precursors. (b) Illustration of the Schlenk flask setup used for the VSIB method. The inset shows the structures of the precursors 1-methylimidazole and 1-bromobutane and the resulting IL [bmim]Br.

Using this approach, [bmim]Br was successfully formed in the ZIF-8 cages, as confirmed by solution ^{1}H NMR of the acid-digested product (Figure 2a; for peak assignments, see Figure S2). Unreacted precursor molecules and [bmim]Br attached to the ZIF-8 surface were removed by washing in ethanol at room temperature. This washing step did not remove the [bmim]Br trapped inside the cages. ^{1}H NMR reveals an average loading of 2.7 [bmim]Br ion pairs per ZIF-8 cage (ip/c). To confirm the complete removal of surface-adsorbed [bmim]Br, samples of the MOF material were taken after each washing step and analyzed by ^{1}H NMR, showing a constant [bmim]Br content from the second washing step onwards (Figure S3). Thermogravimetric analysis (TGA) reveals a mass loss of 28 wt% when the composite is heated to 300 °C. Under these conditions, the ZIF-8 host remains intact (Figure 2b), while the [bmim]Br guest dequaternizes to form volatile alkylimidazoles and alkylbromides.[34] The observed mass loss is in good agreement with the loading calculated from NMR data (2.7 ip/c corresponds to 30 wt%). Powder X-ray diffraction of the product shows the retention of the crystallinity of the ZIF-8 host upon loading (Figure 2c). Furthermore, the increase of the intensity of the (200) and (211) diffraction peaks relative to the (110) reflection is indicative of the [bmim]Br loading; a similar effect was previously observed for the loading of anthracene into ZIF-8.[26] Physisorption at 77 K reveals a lower amount of adsorbed nitrogen for the composite compared to empty ZIF-8, corresponding to a reduction of the BET specific surface area from 1671 to 411 m^2/g (Figure 2d).

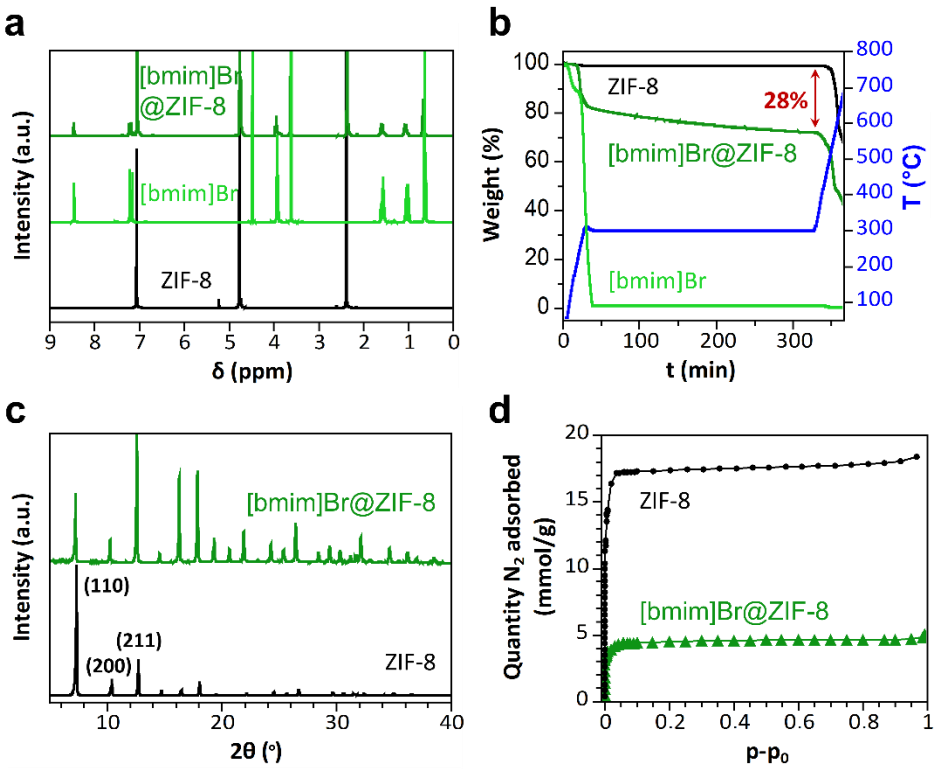

Figure 2. Characterization of [bmim]Br@ZIF-8 obtained by VSIB method. (a) ^{1}H NMR spectrum of ZIF-8 and [bmim]Br@ZIF-8 in DCl/D_2O. (b) TGA of ZIF-8, [bmim]Br@ZIF-8, and [bmim]Br (bulk, for comparison). (c) PXRD patterns of ZIF-8 and [bmim]Br@ZIF-8. (d) N_2 physisorption isotherms of ZIF-8 and [bmim]Br@ZIF-8 at 77 K. The BET specific surface areas of ZIF-8 and [bmim]Br@ZIF-8 are 1671 m^2/g and 411 m^2/g, respectively.

A shorter reaction time (4 h *vs.* 20 h) resulted in a lower IL loading (1.9 ip/c), whereas a prolonged reaction (43 h) did not increase the loading beyond 2.7 ip/c (Figure 3a). Large ZIF-8 crystals (100-300 μm) obtained by solvothermal synthesis were also successfully loaded with [bmim]Br after 20 h of reaction. However, because of diffusion limitations, an overall loading of only 1.6 ip/c could be reached (Figure 3a). When the large crystals were ground into smaller particles, the same loading of 2.7 ip/c as for the smaller crystals was obtained. For the intact large

crystals, the [bmim]Br loading did not change during the washing steps, indicating that all IL was present within the MOF cages and no surface-adsorbed [bmim]Br was formed. Therefore, the washing step could be replaced by simply heating the sample to 120 °C in vacuum to remove unreacted precursors, as confirmed by ^{1}H NMR.

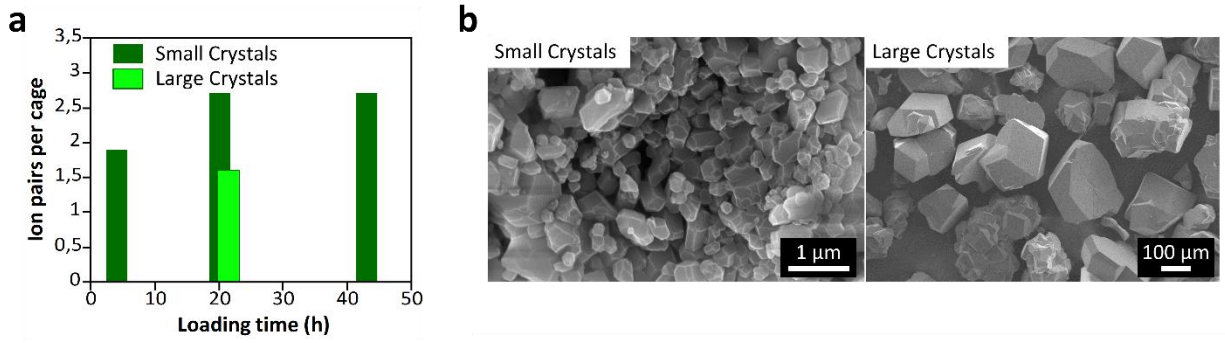

Figure 3. Influence of ZIF-8 crystal size on the IL loading. (a) Number of IL ion pairs obtained per cage of ZIF-8. (b) SEM images of small and large ZIF-8 crystals applied in VSIB experiments.

The removal of [bmim]Br without damaging the ZIF-8 host is illustrated in Figure 4a. Although the [bmim]Br@ZIF-8 composite is stable in ethanol at room temperature, the IL guest can be removed by stirring in hot ethanol (70 °C) for 2 days. Upon heating, the ZIF-8 aperture increases, allowing the IL to diffuse out of the cage.[35,36] Throughout this treatment, ZIF-8 remains crystalline, and the relative intensities of the diffraction peaks are in agreement with the XRD pattern for pristine ZIF-8 (Figure 4b). Furthermore, as observed in the TGA analysis, [bmim]Br could also be removed by heating to 300 °C in nitrogen, via dequaternization to volatile alkylimidazoles and alkylbromides (Figure 4b). Heating unloaded ZIF-8 as a control experiment did not result in any mass loss nor in a loss of crystallinity.

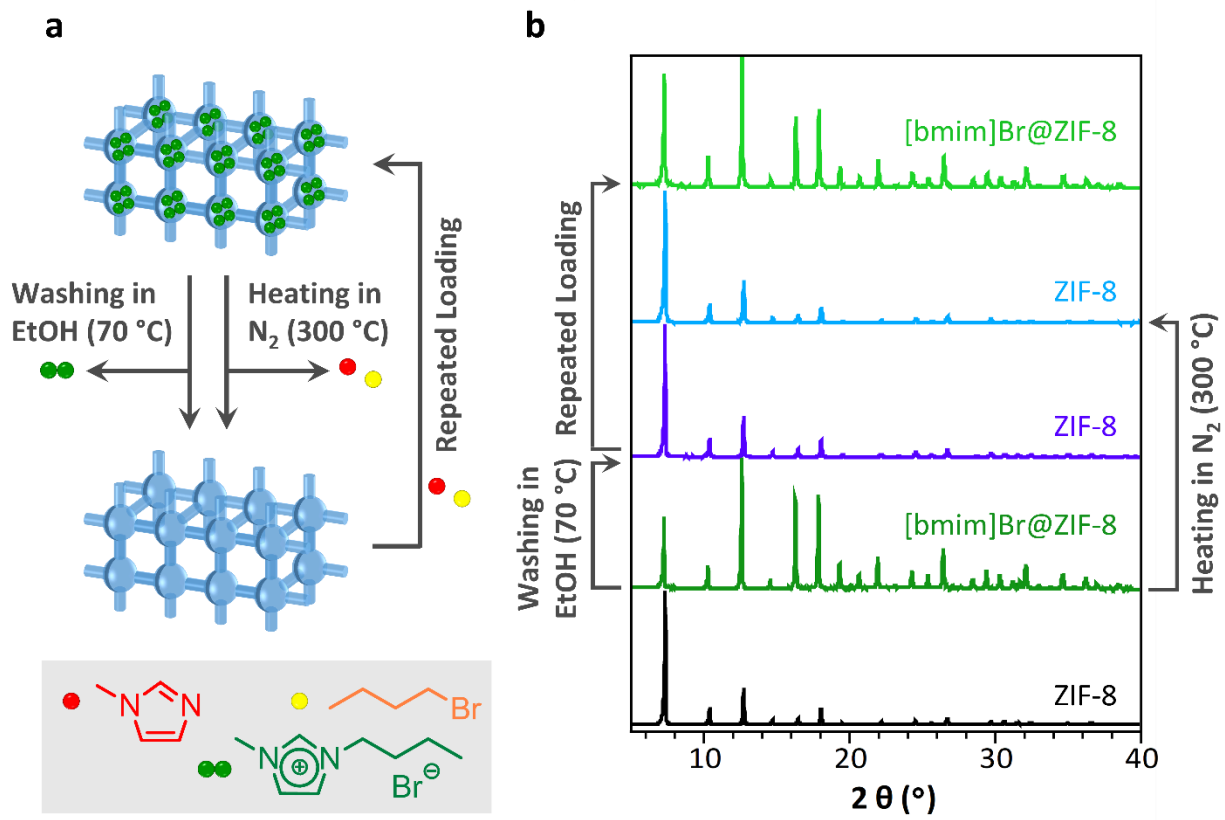

Figure 4. Reversibility of VSIB IL loading. (a) [bmim]Br can be removed from ZIF-8 by washing in EtOH at 70 °C or by heating in nitrogen at 300 °C. ZIF-8 from which the IL has been removed can be loaded using the VSIB method equally well as pristine material. (b) XRD patterns of ZIF-8 (size <1 µm), [bmim]Br@ZIF-8 (2.7 ip/c), after washing in ethanol at 70 °C, after heating at 300 °C in N_2 stream, and [bmim]Br@ZIF-8 (repeated loading after washing out [bmim]Br in ethanol, 2.8 ip/c).

The VSIB method could be extended to ZIF-8 films, which will facilitate the valorization of IL@MOF composites in microelectronics, ionic conductors, or microbatteries. Since both the MOF film and the IL can be deposited from the vapor phase, this approach meets the requirements of microtechnology fabrication (e.g., conformal, defect-free coatings with a controlled thickness).

Loading was performed in a Schlenk flask containing the ZIF-8 film and the IL precursors in separate glass boats at 70 °C (Figure S4). After loading with [bmim]Br, the film was heated to 110 °C to remove unreacted precursor molecules. Grazing-incidence X-ray diffraction demonstrates the crystallinity of the film (Figure 5a) and the change of the relative diffraction intensities indicates the presence of [bmim]Br. As indicated by time-of-flight secondary ion mass spectrometry (ToF-SIMS) depth profiling, [bmim]Br is homogeneously distributed over the ZIF-8 film thickness: a constant signal of $C_8H_{15}N_2^+$ is detected upon sputtering until reaching the film-substrate interface (Figure 5b). Ellipsometry was used to determine the refractive index of the ZIF-8 film before and after IL loading. The [bmim]Br@ZIF-8 film has a refractive index of 1.426, considerably higher than that of the unloaded ZIF-8 film (1.351). The amount of [bmim]Br was calculated to be in the range of 2.8—3.4 ip/c (see Experimental Section), which is similar to the value obtained for the powder samples. Ellipsometric porosimetry using methanol as a probe molecule[37] reveals a lower porosity for the [bmim]Br@ZIF-8 film compared to the unloaded ZIF-8 film, as would be expected (Figure 5c).

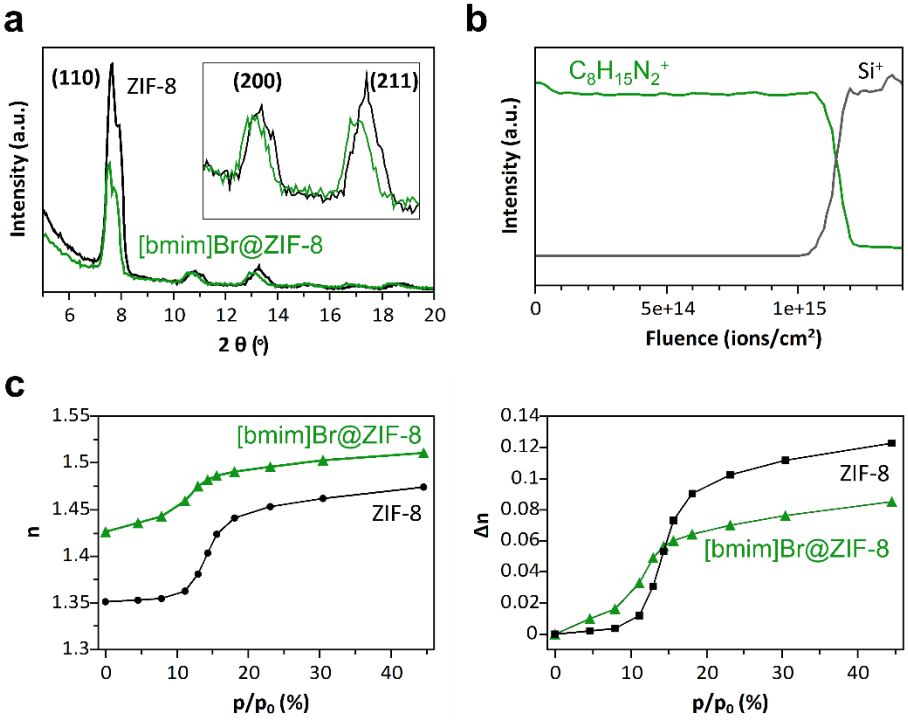

Figure 5. Characterization of [bmim]Br@ZIF-8 films obtained by the VSIB method. (a) GIXRD patterns of ZIF-8 and [bmim]Br@ZIF-8 films (inset: magnified GIXRD 2θ = 9.5—14.5). (b) ToF-SIMS depth profile of [bmim]Br@ZIF-8 film. (c) Methanol adsorption isotherms of ZIF-8 and [bmim]Br@ZIF-8 films; refractive index determined by ellipsometric porosimetry (left: n; right: Δn).

CONCLUSION

We have developed a novel vapor-phase approach for the preparation of [bmim]Br@ZIF-8 composites. Simultaneous diffusion of the precursor vapors into the cages of ZIF-8 leads to the formation of the target IL. This way, efficient solvent-free, vapor-phase loading is enabled and problems related to the low vapor pressure of the target IL are bypassed. In contrast to the conventional SIB method in the liquid phase,[23,24] this vapor-phase approach requires only one step, avoids laborious washing, and is compatible with microfabrication methods.

EXPERIMENTAL SECTION

Materials. ZnO (particle size 25 nm) was purchased from Roth, 2-methylimidazole from Sigma Aldrich, zinc nitrate hexahydrate, 1-bromobutane, and sodium formate from Acros Organics, and 1-methylimidazole from Alfa Aesar and used without further purification.

Characterization. *^{1}H NMR* spectra were recorded on a Bruker Advance 300 MHz spectrometer. The ZIF-8 samples (ca. 5 mg) were dissolved in a solution containing DCl/D_2O (32 wt%, 50 µL) and 500 µL D_2O or acetone-d_6. The loading amount (x) of [bmim]Br (ion pairs per cage) was calculated by equation 1:

$$x = 12\frac{Integral\ of\ [bmim]Br}{Integral\ of\ ZIF{-}8\ linker} \quad (1)$$

TGA was carried out on a STA 449 *F3 Jupiter*® instrument in nitrogen atmosphere (heating to 300 °C at 10 °C/min, isothermal heating at 300 °C for 5 h, heating to 700 °C at 10 °C/min). The correlation between TGA mass loss and loading amount (x) of [bmim]Br is given by equation 2:

$$Mass\ loss = \frac{219x}{219x+1378} \quad (2)$$

Where the molar masses of [bmim]Br and one ZIF-8 cage are 219 g/mol and 1378 g/mol, respectively.

XRD measurements were performed on a Malvern PANalytical Empyrean diffractometer equipped with a PIXcel3D solid-state detector using a Cu anode.

SEM photographs were acquired on an FEI XL30FEG instrument after sputter-coating the samples with 5 nm of Pt.

N_2 sorption isotherms were measured at 77 K using a Micromeritics 3Flex physisorption instrument. The samples were degassed before measurements at 120 °C under dynamic vacuum (10^{-2} mbar) for 3 h.

FTIR measurements were performed on a Varian 670 Fourier Transform-IR spectrometer with a Ge crystal plate in the VeeMAX III module, operated on attenuated total reflection geometry. A liquid-nitrogen-cooled cooled mercury cadmium telluride detector was used.

ToF-SIMS analysis was performed on a TOF.SIMS 5 instrument (ION-TOF GmbH). A 30 keV Bi_3^+ analysis beam (target current: 0.35 pA) was used in a high-current bunched mode for high mass resolution (m Δm^{-1} ~ 8000 at 29 u, $^{29}Si^+$). The primary ion dose was kept sufficiently low so that the static limit of 1×10^{13} ions cm^{-2} per analysis was not exceeded. During measurements, the pressure in the chamber was ~ 3.4×10^{-8} mbar. Depth profiles were obtained in a dual-beam configuration, where a 10 keV Ar_{1250}^+ cluster ion beam (target current: 4.5 nA) was applied as a sputter beam. At the center of the 800 µm × 800 µm crater, a 100 µm × 100 µm area was analyzed.

Spectroscopic ellipsometry was applied to determine the optical properties of unloaded and loaded ZIF-8 thin films by using an iSE instrument (J. A. Woollam, US). Ψ and Δ were recorded from 400 to 1000 nm at a 70° incident angle. Optical modelling was performed using the CompleteEASE 6.60 software (J. A. Woollam, US). A Porous Effective Medium Approximation (Porous EMA) model was used to estimate the pore filling factor of IL within ZIF-8. First, the unloaded ZIF-8 film was measured and modelled using a Cauchy model ($n(\lambda) = A + B/\lambda^2$; k=0) to determine the A and B coefficients of empty ZIF-8. The porosity, ϕ_{por} =58.8 %, was assumed according to reference[38] and the filling factor was kept at zero. For the IL-loaded sample, a Cauchy model was used to model the IL by applying the refractive index of pure IL, A=1.54.[39] The dispersion factor B was either fixed at zero or fitted, which gave about 10 % variation in the fitted filling factor value. The Cauchy coefficients of ZIF-8 were kept constant during the modelling of IL loading. The estimated filling factor was in the range from 27 % to 37 %, which is in a good

agreement with the 34 % methanol uptake reduction upon IL loading (Figure 5c). The loading in mmol/g was calculated by equation 3:

$$\frac{n_{IL}}{m_{ZIF8}} = \frac{V_{IL}}{V_{ZIF8}} \frac{\rho_{IL}\,\phi_{por}}{M_{IL}\,\rho_{ZIF8}} \quad (3)$$

Where $\frac{V_{IL}}{V_{ZIF8}}$ is the filling factor and M_{IL} is the molar mass of IL. The density of ZIF-8 (ρ_{ZIF8} =0.95 g cm^{-3}) was taken from [38]. The density of IL (ρ_{IL} =1.30 g cm^{-3}) was taken from [39]. The loading in ip/c was calculated by assuming the unit cell volume of 4.924 nm^3.[40] Methanol adsorption isotherms of unloaded and IL-loaded films were measured using the iSE in combination with a stainless steel in-situ gas cell and home-build vapour dosing equipment.[41]

Synthesis of ZIF-8. *Powder, small crystals:* ZnO (162 mg, 2.00 mmol) and 2-methylimidazole (481 mg, 5.85 mmol) were mixed and ground with a pestle and mortar. The mixture was heated at 110 °C in a synthesis oven for 1 d, washed with methanol 3 times, and subsequently dried. *Powder, large crystals:* The procedure described in [42] was followed. $ZnNO_3$*$6H_2O$ (3.528 g, 11.86 mmol) was dissolved in 40 mL of methanol; 2-methylimidazole (1.944 g, 23.72 mmol) and sodium formate (0.807 g, 11.86 mmol) were dissolved in 40 mL of methanol. Both solutions were sonicated for 2 minutes, and the latter solution was poured into the former solution under stirring. The reaction mixture was stirred for 2 more min and heated at 90 °C for 24 h in a sealed glass jar. The resulting crystals were removed from the wall by sonication, washed 3 times with methanol, and subsequently dried. *ZIF-8 films:* ZIF-8 thin films were synthesized using the deposition route described in [43]. A 25x25 mm^2 silicon wafer was used as the substrate. Prior to ZIF-8 deposition, the substrate was cleaned in piranha solution (H_2SO_4:H_2O_2 in 3:1 volume ratio) for 30 min at 70 °C and extensively washed with deionized water and methanol. Stock solutions of 25 mM zinc nitrate hexahydrate (Alfa Aesar, 99%) and 50 mM 2-methylimidazole (Acros Organics, 99%) were prepared separately in methanol. The ZIF-8 layer deposition proceeded by combining 10 mL of

each stock solution in a glass beaker and putting the substrate in the reaction mixture facing down. About 5 mm thick plastic spacer ring was used to provide space between the bottom of the beaker and the substrate surface. After 30 minutes of reaction time the substrate was taken out of the reaction mixture and washed in methanol. The deposition step was repeated three times in total to yield 310 nm thick ZIF-8 film. After the last layer deposition, the substrate was sequentially washed 3-times in methanol and once in ethanol, before drying under nitrogen flow.

Vapor-phase loading of IL into ZIF-8. *Powder:* ZIF-8 (100 mg) was weighed into a glass boat, and 1-methylimidazole and 1-bromobutane (0.5 mL each) were filled into glass boats using a pipette. The 3 glass boats were transferred into a Schlenk tube (Figure S1), which was purged with nitrogen to achieve an inert atmosphere, placed in a synthesis oven, and heated at 70 °C for 20 h. Subsequently, the ZIF-8 was washed by stirring in ethanol 4 times (10min—10min—1h—1h), see Figure S3, and dried at 60 °C. The precursor/ZIF-8 ratio of 5 μL/mg could be reduced to 1 μL/mg, resulting in the same loading; a ratio of 0.5 μL/mg still resulted in a loading of 2.3 ip/c. *Film:* The ZIF-8 film and the precursor vials (each containing 5 μL precursor) were glued on a glass slide. The glass slide was transferred into a Schlenk tube (Figure S4), which was purged with nitrogen to achieve an inert atmosphere, placed in a synthesis oven and heated to 70 °C for 3 h. Subsequently, the ZIF-8 film was removed from the Schlenk vial and heated to 110 °C for 1 h to remove unreacted precursor molecules.

ASSOCIATED CONTENT

Supporting Information: Photographs of experimental setups; characterization of bmimBr@ZIF-8 powder samples (^{1}H NMR, FTIR); additional experimental details

AUTHOR INFORMATION

Corresponding author

Rob Ameloot - Center for Membrane Separations, Adsorption, Catalysis, and Spectroscopy (cMACS), KU Leuven, Leuven, Belgium. Email: rob.ameloot@kuleuven.be

Author Contributions

The manuscript was written through contributions of all authors. All authors have given approval to the final version of the manuscript.

ACKNOWLEDGMENTS

We acknowledge funding from the European Union in the Horizon 2020 FETOPEN-1-2016-2017 research and innovation program (grant agreement 801464) and from the Research Foundation Flanders (FWO Vlaanderen) in research and infrastructure projects G0E6319N and I014018N. M.L.T. thanks the FWO for support by a senior postdoctoral fellowship (12ZK720N).

REFERENCES

(1) Kinik, F. P.; Uzun, A.; Keskin, S. Ionic Liquid/Metal-Organic Framework Composites: From Synthesis to Applications. *ChemSusChem* **2017**, *10* (14), 2842–2863. https://doi.org/10.1002/cssc.201700716.

(2) Yoshida, Y.; Kitagawa, H. Ionic Conduction in Metal–Organic Frameworks with Incorporated Ionic Liquids. *ACS Sustainable Chemistry & Engineering* **2019**, *7* (1), 70–81. https://doi.org/10.1021/acssuschemeng.8b05552.

(3) Thomas, A.; Prakash, M. Ionic Liquid Incorporation in Zeolitic Imidazolate Framework-3 for Improved CO2 Separation: A Computational Approach. *Applied Surface Science* **2021**, *562*, 150173. https://doi.org/10.1016/j.apsusc.2021.150173.

(4) Zhao, M.; Ban, Y.; Yang, W. Assembly of Ionic Liquid Molecule Layers on Metal–Organic Framework-808 for CO2 Capture. *Chemical Engineering Journal* **2022**, *439*, 135650. https://doi.org/10.1016/j.cej.2022.135650.

(5) Kinik, F. P.; Altintas, C.; Balci, V.; Koyuturk, B.; Uzun, A.; Keskin, S. [BMIM][PF $_6$] Incorporation Doubles CO $_2$ Selectivity of ZIF-8: Elucidation of Interactions and Their Consequences on Performance. *ACS Appl. Mater. Interfaces* **2016**, *8* (45), 30992–31005. https://doi.org/10.1021/acsami.6b11087.
(6) Fujie, K.; Otsubo, K.; Ikeda, R.; Yamada, T.; Kitagawa, H. Low Temperature Ionic Conductor: Ionic Liquid Incorporated within a Metal–Organic Framework. *Chem. Sci.* **2015**, *6* (7), 4306–4310. https://doi.org/10.1039/C5SC01398D.
(7) Nozari, V.; Calahoo, C.; Tuffnell, J. M.; Keen, D. A.; Bennett, T. D.; Wondraczek, L. Ionic Liquid Facilitated Melting of the Metal-Organic Framework ZIF-8. *Nat Commun* **2021**, *12* (1), 5703. https://doi.org/10.1038/s41467-021-25970-0.
(8) Deiko, G. S.; Isaeva, V. I.; Kustov, L. M. New Molecular Sieve Materials: Composites Based on Metal–Organic Frameworks and Ionic Liquids. *Petroleum Chemistry* **2019**, *59* (8), 770–787. https://doi.org/10.1134/S096554411908005X.
(9) Sezginel, K. B.; Keskin, S.; Uzun, A. Tuning the Gas Separation Performance of CuBTC by Ionic Liquid Incorporation. *Langmuir* **2016**, *32* (4), 1139–1147. https://doi.org/10.1021/acs.langmuir.5b04123.
(10) Li, H.; Tuo, L.; Yang, K.; Jeong, H.-K.; Dai, Y.; He, G.; Zhao, W. Simultaneous Enhancement of Mechanical Properties and CO2 Selectivity of ZIF-8 Mixed Matrix Membranes: Interfacial Toughening Effect of Ionic Liquid. *Journal of Membrane Science* **2016**, *511*, 130–142. https://doi.org/10.1016/j.memsci.2016.03.050.
(11) Zeeshan, M.; Keskin, S.; Uzun, A. Enhancing CO2/CH4 and CO2/N2 Separation Performances of ZIF-8 by Post-Synthesis Modification with [BMIM][SCN]. *Polyhedron* **2018**, *155*, 485–492. https://doi.org/10.1016/j.poly.2018.08.073.
(12) Mohamedali, M.; Henni, A.; Ibrahim, H. Markedly Improved CO2 Uptake Using Imidazolium-Based Ionic Liquids Confined into HKUST-1 Frameworks. *Microporous and Mesoporous Materials* **2019**, *284*, 98–110. https://doi.org/10.1016/j.micromeso.2019.04.004.
(13) Xu, Q.; Zhang, X.; Zeng, S.; Bai, L.; Zhang, S. Ionic Liquid Incorporated Metal Organic Framework for High Ionic Conductivity over Extended Temperature Range. *ACS Sustainable Chemistry & Engineering* **2019**, *7* (8), 7892–7899. https://doi.org/10.1021/acssuschemeng.9b00543.
(14) Fujie, K.; Yamada, T.; Ikeda, R.; Kitagawa, H. Introduction of an Ionic Liquid into the Micropores of a Metal-Organic Framework and Its Anomalous Phase Behavior. *Angewandte Chemie* **2014**, *126* (42), 11484–11487. https://doi.org/10.1002/ange.201406011.
(15) Chen, L.-H.; Wu, B.-B.; Zhao, H.-X.; Long, L.-S.; Zheng, L.-S. High Temperature Ionic Conduction Mediated by Ionic Liquid Incorporated within the Metal-Organic Framework UiO-67(Zr). *Inorganic Chemistry Communications* **2017**, *81*, 1–4. https://doi.org/10.1016/j.inoche.2017.04.019.
(16) Sun, X.-L.; Deng, W.-H.; Chen, H.; Han, H.-L.; Taylor, J. M.; Wan, C.-Q.; Xu, G. A Metal-Organic Framework Impregnated with a Binary Ionic Liquid for Safe Proton Conduction above 100 °C. *Chemistry - A European Journal* **2017**, *23* (6), 1248–1252. https://doi.org/10.1002/chem.201605215.
(17) Xu, L.; Kwon, Y.-U.; de Castro, B.; Cunha-Silva, L. Novel Mn(II)-Based Metal–Organic Frameworks Isolated in Ionic Liquids. *Crystal Growth & Design* **2013**, *13* (3), 1260–1266. https://doi.org/10.1021/cg301725z.

(18) Xu, L.; Liu, B.; Liu, S.-X.; Jiao, H.; de Castro, B.; Cunha-Silva, L. The Influence of 1-Alkyl-3-Methyl Imidazolium Ionic Liquids on a Series of Cobalt-1,4-Benzenedicarboxylate Metal–Organic Frameworks. *CrystEngComm* **2014**, *16* (46), 10649–10657. https://doi.org/10.1039/C4CE01722F.
(19) Ban, Y.; Li, Z.; Li, Y.; Peng, Y.; Jin, H.; Jiao, W.; Guo, A.; Wang, P.; Yang, Q.; Zhong, C.; Yang, W. Confinement of Ionic Liquids in Nanocages: Tailoring the Molecular Sieving Properties of ZIF-8 for Membrane-Based CO_2 Capture. *Angewandte Chemie International Edition* **2015**, *54* (51), 15483–15487. https://doi.org/10.1002/anie.201505508.
(20) Zhang, Z.-H.; Xu, L.; Jiao, H. Ionothermal Synthesis, Structures, Properties of Cobalt-1,4-Benzenedicarboxylate Metal–Organic Frameworks. *Journal of Solid State Chemistry* **2016**, *238*, 217–222. https://doi.org/10.1016/j.jssc.2016.03.028.
(21) Wang, M.-M.; Wei, Z.; Xu, L.; Liu, B.; Jiao, H. Two Temperature-Controlled Zinc Coordination Polymers: Ionothermal Synthesis, Properties, and Dye Adsorption: Two Temperature-Controlled Zinc Coordination Polymers: Ionothermal Synthesis, Properties, and Dye Adsorption. *European Journal of Inorganic Chemistry* **2018**, *2018* (7), 932–939. https://doi.org/10.1002/ejic.201701161.
(22) Khan, N. A.; Hasan, Z.; Jhung, S. H. Ionic Liquid@MIL-101 Prepared via the Ship-in-Bottle Technique: Remarkable Adsorbents for the Removal of Benzothiophene from Liquid Fuel. *Chemical Communications* **2016**, *52* (12), 2561–2564. https://doi.org/10.1039/C5CC08896H.
(23) Ahmed, I.; Panja, T.; Khan, N. A.; Sarker, M.; Yu, J.-S.; Jhung, S. H. Nitrogen-Doped Porous Carbons from Ionic Liquids@MOF: Remarkable Adsorbents for Both Aqueous and Nonaqueous Media. *ACS Applied Materials & Interfaces* **2017**, *9* (11), 10276–10285. https://doi.org/10.1021/acsami.7b00859.
(24) Khan, N. A.; Bhadra, B. N.; Jhung, S. H. Heteropoly Acid-Loaded Ionic Liquid@metal-Organic Frameworks: Effective and Reusable Adsorbents for the Desulfurization of a Liquid Model Fuel. *Chemical Engineering Journal* **2018**, *334*, 2215–2221. https://doi.org/10.1016/j.cej.2017.11.159.
(25) Ahmed, I.; Adhikary, K. K.; Lee, Y.-R.; Ho Row, K.; Kang, K.-K.; Ahn, W.-S. Ionic Liquid Entrapped UiO-66: Efficient Adsorbent for Gd3+ Capture from Water. *Chemical Engineering Journal* **2019**, *370*, 792–799. https://doi.org/10.1016/j.cej.2019.03.265.
(26) Tu, M.; Reinsch, H.; Rodríguez-Hermida, S.; Verbeke, R.; Stassin, T.; Egger, W.; Dickmann, M.; Dieu, B.; Hofkens, J.; Vankelecom, I. F. J.; Stock, N.; Ameloot, R. Reversible Optical Writing and Data Storage in an Anthracene-Loaded Metal-Organic Framework. *Angewandte Chemie International Edition* **2019**, *58* (8), 2423–2427. https://doi.org/10.1002/anie.201813996.
(27) Hermes, S.; Schröder, F.; Amirjalayer, S.; Schmid, R.; Fischer, R. A. Loading of Porous Metal–Organic Open Frameworks with Organometallic CVD Precursors: Inclusion Compounds of the Type $[L_n M]_a$@MOF-5. *J. Mater. Chem.* **2006**, *16* (25), 2464–2472. https://doi.org/10.1039/B603664C.
(28) Cremer, T.; Killian, M.; Gottfried, J. M.; Paape, N.; Wasserscheid, P.; Maier, F.; Steinrück, H.-P. Physical Vapor Deposition of [EMIM][Tf_2N]: A New Approach to the Modification of Surface Properties with Ultrathin Ionic Liquid Films. *ChemPhysChem* **2008**, *9* (15), 2185–2190. https://doi.org/10.1002/cphc.200800300.

(29) Hekayati, J.; Roosta, A.; Javanmardi, J. On the Prediction of the Vapor Pressure of Ionic Liquids Based on the Principle of Corresponding States. *Journal of Molecular Liquids* **2017**, *225*, 118–126. https://doi.org/10.1016/j.molliq.2016.11.031.
(30) Kamal, A.; Chouhan, G. Investigations Towards the Chemoselective Thioacetaliztion of Carbonyl Compounds by Using Ionic Liquid[Bmim]Br as a Recyclable Catalytic Medium. *Advanced Synthesis & Catalysis* **2004**, *346* (5), 579–582. https://doi.org/10.1002/adsc.200303171.
(31) Große Böwing, A.; Jess, A. Kinetics of Single- and Two-Phase Synthesis of the Ionic Liquid 1-Butyl-3-Methylimidazolium Chloride. *Green Chem.* **2005**, *7* (4), 230–235. https://doi.org/10.1039/B417124A.
(32) Obst, M.; Arnauts, G.; Cruz, A. J.; Calderon Gonzalez, M.; Marcoen, K.; Hauffman, T.; Ameloot, R. Chemical Vapor Deposition of Ionic Liquids for the Fabrication of Ionogel Films and Patterns. *Angew. Chem. Int. Ed.* **2021**, *60* (49), 25668–25673. https://doi.org/10.1002/anie.202110022.
(33) Xiao, Y.; Hong, A. N.; Hu, D.; Wang, Y.; Bu, X.; Feng, P. Solvent-Free Synthesis of Zeolitic Imidazolate Frameworks and the Catalytic Properties of Their Carbon Materials. *Chem. Eur. J.* **2019**, *25* (71), 16358–16365. https://doi.org/10.1002/chem.201903888.
(34) Arellano, I. H. J.; Guarino, J. G.; Paredes, F. U.; Arco, S. D. Thermal Stability and Moisture Uptake of 1-Alkyl-3-Methylimidazolium Bromide. *Journal of Thermal Analysis and Calorimetry* **2011**, *103* (2), 725–730. https://doi.org/10.1007/s10973-010-0992-5.
(35) Zhang, C.; Lively, R. P.; Zhang, K.; Johnson, J. R.; Karvan, O.; Koros, W. J. Unexpected Molecular Sieving Properties of Zeolitic Imidazolate Framework-8. *J. Phys. Chem. Lett.* **2012**, *3* (16), 2130–2134. https://doi.org/10.1021/jz300855a.
(36) Guo, Z.; Zheng, W.; Yan, X.; Dai, Y.; Ruan, X.; Yang, X.; Li, X.; Zhang, N.; He, G. Ionic Liquid Tuning Nanocage Size of MOFs through a Two-Step Adsorption/Infiltration Strategy for Enhanced Gas Screening of Mixed-Matrix Membranes. *Journal of Membrane Science* **2020**, *605*, 118101. https://doi.org/10.1016/j.memsci.2020.118101.
(37) Stassin, T.; Verbeke, R.; Cruz, A. J.; Rodríguez-Hermida, S.; Stassen, I.; Marreiros, J.; Krishtab, M.; Dickmann, M.; Egger, W.; Vankelecom, I. F. J.; Furukawa, S.; De Vos, D.; Grosso, D.; Thommes, M.; Ameloot, R. Porosimetry for Thin Films of Metal–Organic Frameworks: A Comparison of Positron Annihilation Lifetime Spectroscopy and Adsorption-Based Methods. *Adv. Mater.* **2021**, *33* (17), 2006993. https://doi.org/10.1002/adma.202006993.
(38) Tan, J. C.; Bennett, T. D.; Cheetham, A. K. Chemical Structure, Network Topology, and Porosity Effects on the Mechanical Properties of Zeolitic Imidazolate Frameworks. *Proceedings of the National Academy of Sciences* **2010**, *107* (22), 9938–9943. https://doi.org/10.1073/pnas.1003205107.
(39) Kim, K.-S.; Shin, B.-K.; Lee, H. Physical and Electrochemical Properties of 1-Butyl-3-Methylimidazolium Bromide, 1-Butyl-3-Methylimidazolium Iodide, and 1-Butyl-3-Methylimidazolium Tetrafluoroborate. *Korean J. Chem. Eng.* **2004**, *21* (5), 1010–1014. https://doi.org/10.1007/BF02705586.
(40) Hobday, C. L.; Woodall, C. H.; Lennox, M. J.; Frost, M.; Kamenev, K.; Düren, T.; Morrison, C. A.; Moggach, S. A. Understanding the Adsorption Process in ZIF-8 Using High Pressure Crystallography and Computational Modelling. *Nat Commun* **2018**, *9* (1), 1429. https://doi.org/10.1038/s41467-018-03878-6.

(41) Tietze, M. L.; Obst, M.; Arnauts, G.; Wauteraerts, N.; Rodríguez-Hermida, S.; Ameloot, R. Parts-per-Million Detection of Volatile Organic Compounds via Surface Plasmon Polaritons and Nanometer-Thick Metal–Organic Framework Films. *ACS Appl. Nano Mater.* **2022**, *5* (4), 5006–5016. https://doi.org/10.1021/acsanm.2c00012.
(42) Zhang, K.; Lively, R. P.; Zhang, C.; Koros, W. J.; Chance, R. R. Investigating the Intrinsic Ethanol/Water Separation Capability of ZIF-8: An Adsorption and Diffusion Study. *J. Phys. Chem. C* **2013**, *117* (14), 7214–7225. https://doi.org/10.1021/jp401548b.
(43) Lu, G.; Hupp, J. T. Metal−Organic Frameworks as Sensors: A ZIF-8 Based Fabry−Pérot Device as a Selective Sensor for Chemical Vapors and Gases. *J. Am. Chem. Soc.* **2010**, *132* (23), 7832–7833. https://doi.org/10.1021/ja101415b.